Energy 81 (2015) 437–445

Contents lists available at ScienceDirect

Energy

journal homepage: www.elsevier.com/locate/energy

Renewable build-up pathways for the US: Generation costs are not system costs

Sarah Becker [a, b, *], Bethany A. Frew [b], Gorm B. Andresen [c, b], Mark Z. Jacobson [b], Stefan Schramm [a], Martin Greiner [c, d]

[a] Frankfurt Institute for Advanced Studies, Goethe-Universität, 60438 Frankfurt am Main, Germany
[b] Department of Civil and Environmental Engineering, Stanford University, Stanford, CA, USA
[c] Department of Engineering, Aarhus University, 8200 Aarhus N, Denmark
[d] Department of Mathematics, Aarhus University, 8000 Aarhus C, Denmark

ARTICLE INFO

Article history:
Received 6 November 2014
Received in revised form
15 December 2014
Accepted 21 December 2014
Available online 27 January 2015

Keywords:
Energy system design
Large-scale integration of renewable power generation
Renewable power generation
Optimal mix of wind and solar PV
Levelized cost of electricity

ABSTRACT

The transition to a future electricity system based primarily on wind and solar PV is examined for all regions in the contiguous US. We present optimized pathways for the build-up of wind and solar power for least backup energy needs as well as for least cost obtained with a simplified, lightweight model based on long-term high resolution weather-determined generation data. In the absence of storage, the pathway which achieves the best match of generation and load, thus resulting in the least backup energy requirements, generally favors a combination of both technologies, with a wind/solar PV (photovoltaics) energy mix of about 80/20 in a fully renewable scenario. The least cost development is seen to start with 100% of the technology with the lowest average generation costs first, but with increasing renewable installations, economically unfavorable excess generation pushes it toward the minimal backup pathway. Surplus generation and the entailed costs can be reduced significantly by combining wind and solar power, and/or absorbing excess generation, for example with storage or transmission, or by coupling the electricity system to other energy sectors.

1. Introduction

We investigate highly renewable electricity scenarios for the contiguous US. In this paper, the main focus is placed on the optimization of the mix of wind and solar PV power during the renewable build-up. While numerous studies investigate regional or nationwide fully renewable power systems [1–7], they usually focus on detailed single scenarios or pathways and/or only cost-optimal installations. Here, a simplified and computationally lightweight description based on high-resolution wind, solar PV, and load data is used to survey a large number of possible renewable scenarios and derive systematic insights from the spatio-temporal characteristics of the generation-load mismatch.

In our model of the electricity system, the supply is largely reliant on the variable renewable energy sources wind and solar PV power, which we abbreviate as VRES (variable renewable energy sources). CSP (concentrated solar power) is not implemented yet. The rest of the electricity generation is assumed to be dispatchable, and it is implied that it is used to cover the residual demand that remains after VRES generation has been subtracted from the load. From this point of view, the dispatchable part of the power system will be referred to as the backup system, and correspondingly, the energy from this system will be termed backup energy. Examples for backup power plants in a fully renewable setting are hydro-electric power, geothermal power, and to some extent CSP with thermal storage. In general, any other form of dispatchable generation can be used. The share of VRES in the system is measured as gross share, i.e. the total VRES generation divided by the total load. Due to temporal mismatches in generation and load, the VRES net share, i.e. the amount of VRE (variable renewable energy) actually consumed in the electricity system at the time of their generation is generally lower. Even in a system with a VRES gross share of 100%, the load will partly be covered from backup. This renders contributions from dispatchable renewable sources crucial to a fully renewable system.

To get an impression of the dimensions of the installations, current and extrapolated renewable installations are shown in

* Corresponding author. Frankfurt Institute for Advanced Studies, Goethe-Universität, 60438 Frankfurt am Main, Germany.
E-mail address: becker@fias.uni-frankfurt.de (S. Becker).

http://dx.doi.org/10.1016/j.energy.2014.12.056

Tables 1 and 2. Currently, most of the renewable power capacity is hydro power with a total of almost 80 GW in 2012, closely followed by wind with a total of close to 60 GW. Other technologies are dwarfed in comparison, but solar PV power has seen high growth rates over the past years [8]. The largest future renewable potentials are projected to lie in wind and solar power and are claimed to be sufficient to cover the world energy demand [9,10], so we concentrate on these. When extrapolating wind and solar capacities to the point where they reach a gross share of 100%, maximal total capacities as given in the first two columns of Table 2 result. These capacities are theoretical estimates for the total installed capacity in each FERC (Federal Electricity Regulatory Council) region in a hypothetical setting where wind power (first column) resp. solar PV power (second column) alone produces on average what is consumed. It is seen that even in this upper bound case, average installation densities in each FERC region (third and fifth column of Table 2) remain feasible in all regions. Only the most concentrated wind sites in ERCOT and SE, at which maximal wind installation densities of 23.2 MW/km^2 resp. 39.6 MW/km^2 occur (cf. fourth column of Table 2), will need to be redistributed to neighboring grid cells, which should not be a problem viewed in the light of the low average wind installation densities. Solar installation densities remain moderate even at the most concentrated sites, cf. the sixth column of Table 2.

We make a couple of simplifying assumptions: No ramping limits are imposed on the backup system, entailing no surplus generation from backup plants. The slopes in both the load time series and the residual load are given in Table 3. Column 1 gives the average slope in the load (taking no renewable production into account), column 2 is the maximal slope of the load, and column 3 and 4 are the average and maximal slopes of the residual load for the case of 100% wind and solar gross share with a backup energy minimizing wind/solar mix, see Sec. 2.2 for details. All slopes are normalized by the average load. It is seen that while the average slope does not increase much, extreme slopes rise from around 15% of the average load to 70–100% of the average load within 1 h, indicating the need for a more flexible backup system.

Table 1
Currently (2012) installed renewable capacities in the US, as reported by the US Department of Energy [8]. The reference gives the installations on a state basis, and they have been aggregated into FERC regions using the following approximations (FERC borders and state borders often, but not always, coincide, cf. Fig. 1): AllCA (All California) – California; ERCOT (Electricity Regulatory Council of Texas) – Texas; ISONE (Independent System Operator New England) – Maine, New Hampshire, Vermont, Massachusetts, Connecticut, Rhode Island; MISO (Midcontinent Independent System Operator) – North Dakota, South Dakota, Minnesota, Iowa, Missouri, Michigan, Wisconsin, Illinois, Indiana; NW (Northwest) – Washington, Oregon, Idaho, Montana, Wyoming, Nevada, Utah; NYISO (New York Independent System Operator) – New York; PJM (Pennsylvania, New Jersey, Maryland) – Ohio, West Virginia, Virginia, Maryland, Delaware, Pennsylvania, New Jersey; SE (Southeast) – Arkansas, Kentucky, Tennessee, Mississippi, Alabama, Georgia, North Carolina, South Carolina, Florida; SPP (Southwest Power Pool) – Nebraska, Kansas, Oklahoma, Louisiana; SW (Southwest) – Arizona, New Mexico, Colorado. Abbreviations are Geo. – Geothermal, Bm. Biomass. All installed capacities are given in GW.

FERC	Wind	PV	CSP	Geo.	Bm.	Hydro
AllCA	5.54	2.56	0.36	2.7	1.3	10.1
ERCOT	12.21	0.14	0.00	0.0	0.5	0.7
ISONE	0.83	0.29	0.00	0.0	1.7	1.9
MISO	17.79	0.12	0.00	0.0	1.6	4.1
NW	9.47	0.44	0.06	0.6	0.9	36.2
NYISO	1.64	0.18	0.00	0.0	0.5	4.7
PJM	2.48	1.38	0.00	0.0	1.9	2.6
SE	0.03	0.40	0.08	0.0	4.6	13.2
SPP	6.31	0.02	0.00	0.0	0.5	1.3
SW	3.32	1.61	0.04	0.0	0.1	3.4
Total	59.62	7.13	0.55	3.3	13.4	78.16

Additional measures of matching VRES generation and demand, such as storage or demand-side management, are not treated explicitly. Likewise, potential future changes in load characteristics or load flexibility, which may arise e.g. due to electric cars, are not directly taken into account. Whenever VRES generation exceeds the demand, surplus energy production occurs. This surplus is initially assumed to be of no value in our model. The effect of surplus energy being sold, possibly at a lower price, to storage, transmission, or to cover other (partly) flexible demand like electric vehicle charging or synthetic fuel production, is investigated later in this paper. Additionally, sensitivities to different price assumptions are examined.

The core model has been developed and applied to obtain optimal mixes in fully renewable energy systems as well as potential transmission grid extensions by Becker et al. [11]. Here, it is applied to different build-up pathways toward a fully renewable electricity supply.

This paper is starts with a short description of the underlying data and methodology in Sec. 2. Subsequently, the resulting US build-up pathways and their sensitivities to cost assumptions and surplus usage are presented in Sec. 3. Sec. 4 summarizes the main findings and concludes the paper.

2. Data and methodology

2.1. Load and generation data

The analysis is based on weather data for 32 years with one hour time steps and 30 × 30 km^2 grid cells, covering the time span 1979–2010, from the NCEP (National Centers for Environmental Prediction) Climate Forecast System Reanalysis [13]. They were converted to wind and solar PV generation data as described in by Refs. [11,14,15]. Wind capacity layouts were chosen similarly to those used to produce the NREL (National Renewable Energy Laboratory) wind datasets [16,17], while solar PV capacity was distributed according to the potential generation in each grid cell. Solar panels with a nameplate capacity of 156 kW fixed in southward direction at a tilt equal to the latitude were assumed. This tilt implies that the panel orientation is optimal for the average solar noon position. In our data, solar capacity factors between 15% (in ISONE and NYISO) and 20% (in California and SW) are observed. 3 MW wind turbines with a hub height of 80 m onshore and 7 MW at 100 m hub height offshore were assumed, yielding average capacity factors between 23% in SE and 42% in ISONE, see Table 4. Power generation from each grid cell was aggregated to FERC (Federal Electricity Regulatory Council) region level. See Fig. 1 for a map of the contiguous US FERC regions. Details of the data processing can be found in Ref. [11].

Historical load data for the years 2006–2007 were compiled for each FERC region in Ref. [12]. Where necessary, load data were extended by repetition to cover the 32-year simulation period.

The aggregation of wind and solar PV generation as well as load implies that no FERC-region-internal bottlenecks are present in the transmission grid. It is indeed likely that in a highly renewable electricity system, the regional transmission grids will be reinforced, because of the beneficial effects of aggregation on smoothing wind and solar PV output, well documented in the scientific literature, e.g. Refs. [18–24]. Inter-FERC-region transmission has the potential to smooth VRES generation even further [10,11], but is initially not incorporated into the model.

Central to our research is the mismatch Δ_n between load L_n and generation G_n^S, G_n^W from solar PV and wind, respectively, in FERC region n.

Table 2
Estimated maximal installed wind and solar PV power capacities, as well as average and maximal installation densities ρ. These would occur if a VRES gross share of 100% was attained with wind resp. solar PV only. Capacity values are based on 2006/07 load averages.

FERC	max. wind cap./GW	max. PV cap./GW	$\rho^{\text{wind}}_{\text{avg}}/(\text{MW/km}^2)$	$\rho^{\text{wind}}_{\text{max}}/(\text{MW/km}^2)$	$\rho^{\text{PV}}_{\text{avg}}/(\text{MW/km}^2)$	$\rho^{\text{PV}}_{\text{max}}/(\text{MW/km}^2)$
AllCA	130.4	169.1	0.29	8.2	0.41	0.67
ERCOT	149.2	201.5	0.30	23.2	0.40	0.48
ISONE	35.6	98.1	0.11	3.6	0.51	0.58
MISO	222.2	406.4	0.13	2.2	0.26	0.31
NW	105.5	140.7	0.06	2.5	0.08	0.12
NYISO	51.6	126.5	0.29	6.8	0.95	1.19
PJM	220.8	523.5	0.37	8.9	1.04	1.21
SE	530.1	755.1	0.46	39.6	0.65	0.77
SPP	74.7	129.5	0.09	2.4	0.15	0.18
SW	80.8	120.2	0.08	1.9	0.12	0.15

$$\Delta_n(t) = \gamma_n \langle L_n \rangle \left[\left(1 - \alpha_n^{\text{W}}\right) G_n^{\text{S}}(t) + \alpha_n^{\text{W}} G_n^{\text{W}}(t) \right] - L_n(t) \tag{1}$$

In this expression, wind and solar generation are understood to be normalized to an average of one, and then scaled with the mean load $\langle L_n \rangle$ to a given gross share γ_n of the load. The relative share of wind in the VRE generation is denoted α_n^{W}, the corresponding relative share of solar PV is $(1 - \alpha_n^{\text{W}})$.

Note that the VRES gross share γ_n is the ratio between the average VRES production and the average load, not to be confused with the share of VRES electricity in the total consumption, the VRES net share. This is due to the fluctuating nature of VRES generation, which especially for $\gamma_n > 50\,\%$ leads to surplus VRES production that does not contribute to covering the electric load. γ_n is an upper bound on the percentage of VRES in the electricity mix.

2.2. Backup energy-minimal mix

Here, the only concern is to keep the need for backup energy, which is calculated as the sum of negative mismatches throughout all time steps, as small as possible. In other words, the sum of the negative parts (denoted $(\cdot)_-$) of the mismatch in Eq. (1) is minimized as a function of α_n^{W}:

$$\min_{\alpha_n^{\text{W}}} \sum_t (\Delta_n(t))_- \tag{2}$$

The backup energy minimization leading to Fig. 2 is performed independently for different VRE gross shares γ_n. Since in our modeling, the VRE gross share γ_n and hence the total energy produced from VRES is fixed, least backup energy needs are equivalent to least surplus VRES generation. In other words, when minimizing the need for backup energy from dispatchable sources, the VRES surplus energy is minimized at the same time.

When the VRES gross share γ_n is less than 100%, at least a fraction of $(1 - \gamma_n)$ of the demand has to be covered by the backup system, even if no VRES generation comes as surplus energy. The energy provided by the backup system beyond this minimal share is termed additional backup energy, and this is the part of the backup energy that can be reduced by a suitable choice of the wind/solar mix.

2.3. Regional LCOE

Wind and solar PV LCOE (levelized costs of electricity) are expected to vary spatially due to different external conditions. The inhomogeneity is captured by region-specific cost factors in our model. The main cause of deviations is the weather-dependent capacity factor CF_n for each region (indexed n), i.e. the ratio of average generated power to the maximal generator capacity. Since the costs of VRE plants are to a large part installation and maintenance costs which are proportional to the total installed capacity, but almost independent of the total power output, the costs per unit of energy are in good approximation anti-proportional to the total generated energy. Expressed in terms of the capacity factor, this yields a regional weight factor of

$$w_n = \frac{N}{\sum_m 1/CF_m} \cdot \frac{1}{CF_n} \tag{3}$$

The normalization (first factor) is necessary to keep the average of the weights at unity. N is the number of regions, in this case, 10.

The second reason for variations in LCOE in the FERC regions are different labor and material costs, which have been compiled by the

Table 3
Slopes of the part of the electrical load to be covered by the backup system, for the case of no wind and solar production (first two columns, $m^{(L)}$), and the case of 100% wind and solar gross share (third and fourth column, $m^{(R)}$). The wind/solar ratio in the latter case is determined as the backup energy minimizing mix, cf. Sec. 2.2. Shown are average (subscript "avg") as well as maximal (subscript "max") values. All slopes are normalized by the mean load in their respective FERC region.

FERC	$m^{(L)}_{\text{avg}}$	$m^{(L)}_{\text{max}}$	$m^{(R)}_{\text{avg}}$	$m^{(R)}_{\text{max}}$
AllCA	0.04	0.16	0.05	0.92
ERCOT	0.04	0.19	0.06	0.87
ISONE	0.04	0.17	0.06	0.81
MISO	0.03	0.13	0.05	0.74
NW	0.03	0.14	0.05	0.63
NYISO	0.03	0.15	0.06	0.72
PJM	0.03	0.14	0.05	0.75
SE	0.04	0.14	0.05	0.72
SPP	0.03	0.21	0.05	0.94
SW	0.03	0.14	0.05	0.99

Table 4
Relative regional LCOE (levelized costs of electricity) for the 10 FERC regions, for solar (left) and wind (right), together with the capacity factor CF_n, resource-quality related weight factor w_n (see Eq. (3)), and regional material and labor cost weights c_n (from Ref. [25]). Cost differences due to building in easier accessible or more remote areas are not presently included.

Region	CF_n	w_n	c_n	Rel. LCOE_n	Region	CF_n	w_n	c_n	Rel. LCOE_n
AllCA	0.20	0.87	1.04	89.8%	AllCA	0.25	1.15	1.04	119.5%
ERCOT	0.18	0.98	0.97	94.0%	ERCOT	0.24	1.24	0.97	120.0%
ISONE	0.15	1.12	1.02	113.5%	ISONE	0.42	0.70	1.02	71.0%
MISO	0.17	1.03	1.01	103.6%	MISO	0.30	0.97	1.00	96.8%
NW	0.19	0.91	1.00	90.4%	NW	0.25	1.17	1.00	116.9%
NYISO	0.15	1.15	1.10	125.6%	NYISO	0.36	0.80	1.04	83.6%
PJM	0.16	1.10	1.03	112.8%	PJM	0.37	0.80	1.01	80.5%
SE	0.16	1.05	0.94	98.2%	SE	0.23	1.27	0.98	124.0%
SPP	0.18	0.94	0.96	90.0%	SPP	0.31	0.93	0.98	91.5%
SW	0.20	0.84	0.98	82.1%	SW	0.30	0.97	0.99	96.2%
Avg.	0.17	1.00	1.00	100.0%	Avg.	0.30	1.00	1.00	100.0%

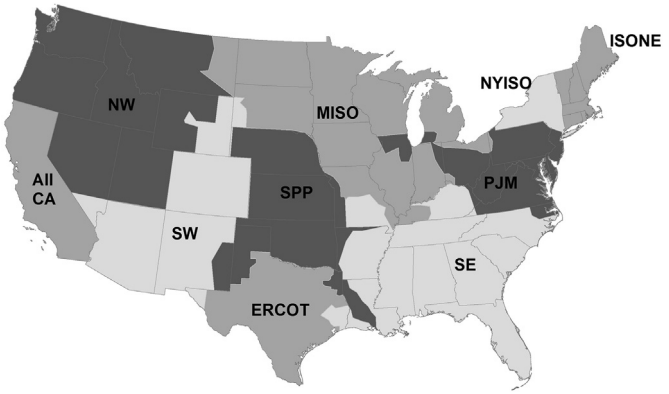

Fig. 1. FERC (Federal Electricity Regulatory Council) regions of the contiguous US, based on [12].

US Army Corps of Engineers [26], and adapted to the problem at hand in Energy and Environmental Economics [25]. These yield another factor c_n of the order of one, which modifies the regional LCOE. The accessibility of the average site in each region is another factor that can influence installation and maintenance costs, but is not accounted for here. Taken together, the regional LCOE are calculated as:

$$\mathrm{LCOE}_n = w_n c_n \mathrm{LCOE}_{\mathrm{avg}} \tag{4}$$

They are determined separately for wind and solar PV. The capacity factor weights w_n as well as the regional cost factors c_n are given in Table 4, which also shows the relative LCOE in the different FERC regions, for solar PV and wind power separately.

As a rough guess, we assume equal wind and solar PV $\mathrm{LCOE}_{\mathrm{avg}}$ of \$0.04/kWh. This choice is in accordance with the most recent Lazard LCOE estimates [27], reporting 2014 unsubsidized LCOE for wind in the range \$0.031–\$0.087/kWh and for utility scale solar PV \$0.072–\$0.086/kWh. Given that the renewable shares discussed in this paper represent mid- to far-future scenarios, and the steeper historical LCOE reductions for solar PV as compared to wind, the assumption of \$0.04/kWh for both appears reasonable. It should be noted that our results depend only on the relative costs of wind and solar PV (with the obvious exception of the future absolute LCOE), and so remain valid even if LCOE see a slightly different development. Furthermore, we have investigated the effect of LCOE changes in a sensitivity analysis (Sec. 3.4).

2.4. LCOE-minimal mix

For each region n, the local wind and solar PV LCOE resulting from the regionalization, Eq. (4), are combined into an average regional LCOE of VRES, depending on the relative wind share in VRES, α_n^{W}:

$$\mathrm{LCOE}_{0,n}\left(\alpha_n^{\mathrm{W}}\right) = \alpha_n^{\mathrm{W}} \mathrm{LCOE}_n^{\mathrm{W}} + \left(1-\alpha_n^{\mathrm{W}}\right)\mathrm{LCOE}_n^{\mathrm{S}}$$

These are then modified to account for the effects of surplus production: It is initially assumed that the surplus production has no value and thus effectively raises LCOE by reducing the amount of usable electric energy produced, as stated in Eq. (5) below.

$$\mathrm{LCOE}_{\mathrm{mod.},n}\left(\alpha_n^{\mathrm{W}}\right) = \mathrm{LCOE}_{0,n}\left(\alpha_n^{\mathrm{W}}\right) \cdot \frac{E_{\mathrm{generated}}\left(\alpha_n^{\mathrm{W}}\right)}{E_{\mathrm{generated}}\left(\alpha_n^{\mathrm{W}}\right) - E_{\mathrm{surplus}}\left(\alpha_n^{\mathrm{W}}\right)} \tag{5}$$

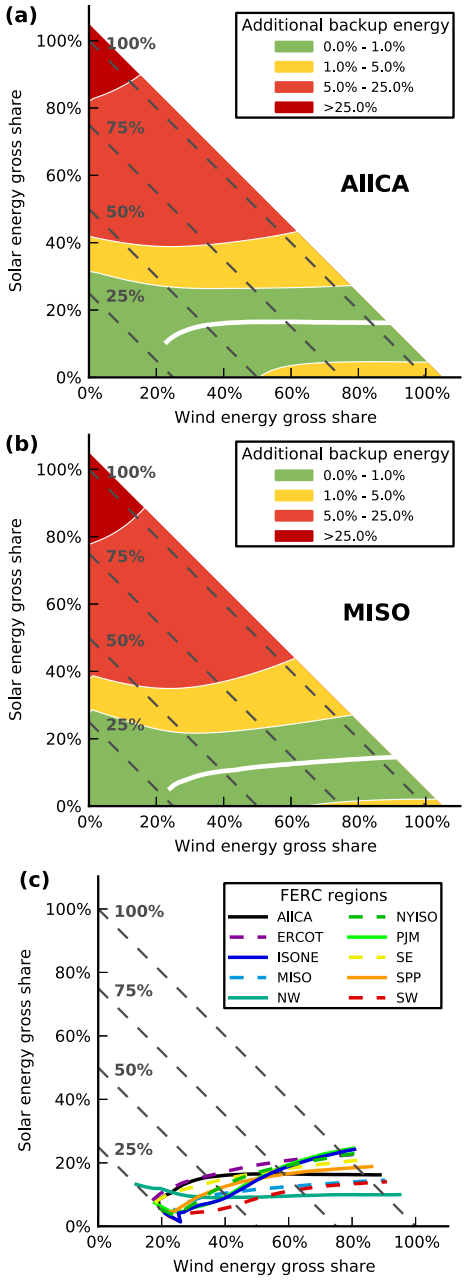

Fig. 2. (a), (b): Build-up pathway from a renewable gross share of 0 % to 100 % for (a) California and (b) MISO that minimizes backup energy needs (Eq. (2) in Sec. 2.1) during the entire renewable build-up. In each of these plots, the white line indicates the build-up pathway minimizing backup energy requirements at the later stages of the installation process. In the green region, backup energy is up to 1 percentage point (pp) of the load larger than optimal. In the yellow region, it is up to 5 pp larger than optimal. In the light red region, it is up to 25 pp larger, and in the dark red region, more than 25 pp larger. The dark gray dashed lines indicate renewable gross shares γ_n of 25 %, 50 %, 75 %, and 100 %. (c): Build-up pathways minimizing backup energy for all FERC regions, analogous to the white line in (a) and (b), starting from 25 % VRE gross share. For lower shares, the minimum in backup energy as a function of wind/solar mix is very shallow. This leads to fluctuations in the optimal mix as a function of VRE gross share, which are not indicative. The optimal mix is therefore only shown above a VRE share of 25 %. (For interpretation of the references to color in this figure legend, the reader is referred to the web version of this article.)

$E_{\mathrm{generated}}$ is the total energy generated from VRES, and E_{surplus} is the VRES surplus energy. Notice that the amount of surplus energy here equals the amount of additional backup energy requirements due to VRES fluctuations, discussed in the section above.

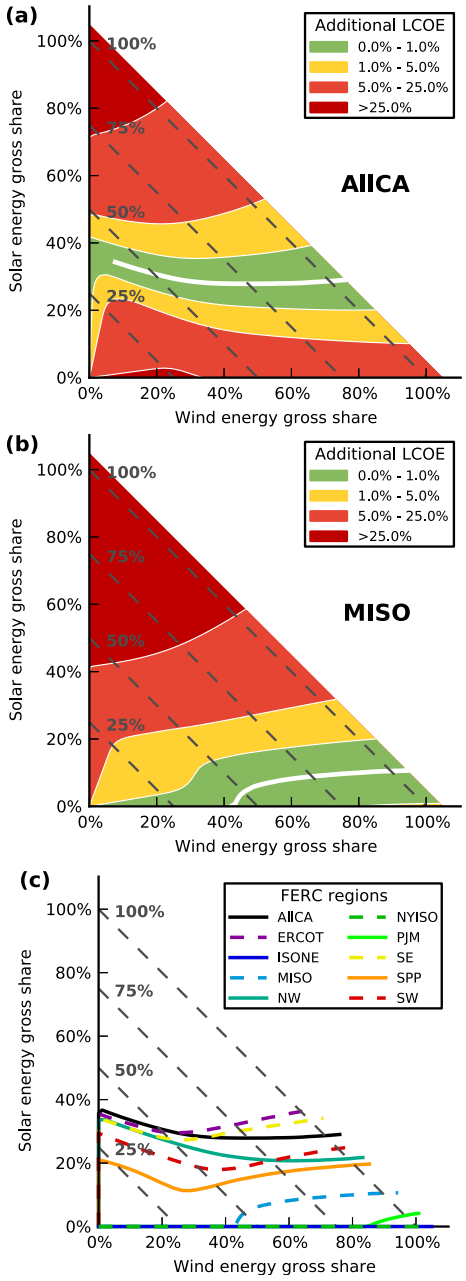

Fig. 3. (a), (b): Build-up pathway from a renewable gross share of 0 % to 100 % for (a) California and (b) MISO that minimizes combined renewable LCOE (Eq. (5)) during the entire renewable build-up. In each of these plots, the white line indicates the build-up pathway minimizing LCOE at the later stages of the installation process. In the green region, LCOE are up to 1 percentage point (pp) larger than optimal, in the yellow region, up to 5 pp, in the light red region, up to 25 pp, and in the dark red region, more than 25 pp larger. The dark gray dashed lines indicate renewable gross shares γ_n of 25 %, 50 %, 75 %, and 100 %. LCOE are assumed to be equally $0.04/kWh for both wind and solar PV on average across the contiguous US, which translates into $0.048/kWh for wind and $0.036/kWh for solar PV in California and $0.039/kWh for wind and $0.041/kWh for solar PV in MISO when LCOE are regionally adjusted, see Eq. (4). (c): LCOE-minimal build-up pathways for all FERC regions, analogous to the white lines in (a) and (b). Note that since the LCOE-minimal mix for ISONE and NYISO is 100 % wind during the entire build-up, their pathways coincide with the x-axis. (For interpretation of the references to color in this figure legend, the reader is referred to the web version of this article.)

3. Results

3.1. Minimal backup energy pathways

Backup energy minimizing build-up pathways have been calculated by optimizing the wind/solar mix for VRE gross shares between 0% and 100%, see Eq. (2) in Sec. 2.1. Detailed examples are shown in Fig. 2a for California and in Fig. 2b for MISO. The minimizing pathways for all other FERC regions are included in Fig. 2c. Fig. 2a and b presents the optimal pathway (white line), along which backup energy is minimal for each given VRES share. Additionally, parameter combinations that lead to increasingly more backup energy than the optimal path are indicated: In the green region, the average backup energy requirement is less than 1 pp (percentage point) of the average load more than optimal, in the yellow region, 5 pp, in the red region, 25 pp, and in the dark red region, more than 25 pp. The green region is seen to successively shrink during the build-up, showing that the minimum in backup energy becomes more and more pronounced with growing VRE share. This observation is corroborated by Fig. 4a and c, where sections for several fixed renewable gross shares through the backup energy needs are shown as a function of the wind/solar mix. Only additional backup energy is included in Fig. 4a and c, which arises due to VRE fluctuations. It is equal to the excess of backup

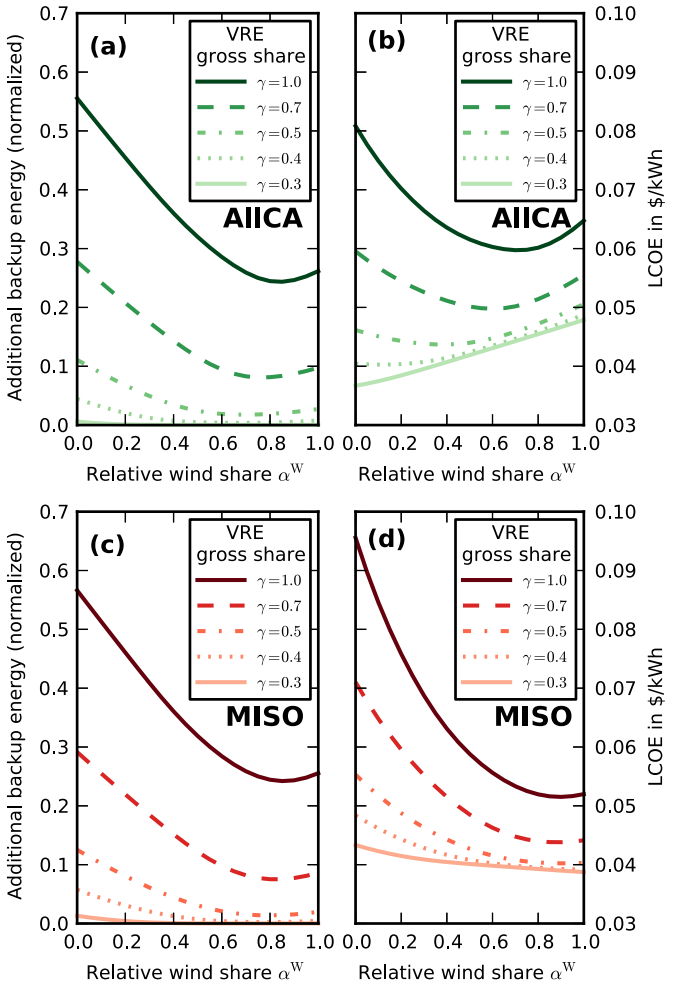

Fig. 4. (a), (c): Additional backup energy, normalized by the average load, and (b), (d): LCOE as a function of the wind/solar mix, for different VRES gross shares γ between 30 % and 100 %, in the example FERC regions (a), (b) AllCA and (c), (d) MISO.

energy over the expected "missing energy" of total electricity demand minus total VRES generation; see Sec. 2.1 for details.

In the early stage of VRE installations, until wind and solar PV cover about 30% of the load, the sensitivity of backup energy need with respect to the mix of wind and solar is relatively low, because both wind and solar PV generation hardly ever exceed the demand, so all energy they produce can be used in the electricity system and no additional backup energy is required. Toward a fully renewable system, the mismatch between load and generation grows. Once VRE gross shares reach 30%–50%, substantial VRE surplus generation and hence need for additional backup energy at other times occurs, which can be minimized using the mix of wind and solar PV as a handle. During the later stages of the development, when VRE gross shares reach more than 50%, backup minimal mixes for all FERC regions are observed around 80% wind and 20% solar PV, with a spread of about 10% across the different FERC regions, cf. Fig. 2c.

3.2. Minimal LCOE pathways

LCOE-optimized VRES build-up paths are shown in Fig. 3a for the example of California and in Fig. 3b for MISO in detail, and similar pathways in Fig. 3c for all FERC regions. As above, the white line traces the optimal path. Here, the green region indicates scenarios in which LCOE are up to 1 pp of the average of wind and solar PV LCOE (before the modifications of Eq. (5)) higher than optimal. In the yellow region, LCOE are up to 5 pp higher than optimal, in the light red region, up to 25 pp, and in the dark red region, more than 25 pp. All pathways are calculated under the example assumption of equal country-average VRES LCOE for wind and solar PV of \$0.040/kWh. With the cost regionalization of Eq. (4), this yields \$0.048/kWh for wind and \$0.036/kWh for solar PV in California and \$0.039/kWh for wind and \$0.041/kWh for solar PV in MISO.

In contrast to the backup optimal pathways of Fig. 2a–c, the LCOE optimal mix strongly favors the lower cost technology for low renewable penetrations – solar PV for California, wind for MISO under our example cost assumptions. The cause for this behavior is that both can be integrated equally well into the system, so there is no disadvantage in picking the cheaper one. Only when surplus production and additional backup requirements become more prominent and expensive, around VRES gross shares of 30%–50%, the mix shifts toward lower backup energy requirements. This effect is further illustrated in Fig. 4b and d, where the shift of the LCOE minimum from least generation cost for low VRE gross shares toward least surplus/additional backup for higher shares is clearly visible. It can be interpreted as an indication that although in the short run it appears cheaper to settle for the lower generation cost resource, in the long run it pays to sustain a mixed portfolio, which is able to reduce backup energy needs and surplus production.

It is interesting to compare the build-up pathway for California obtained here to the results of the more detailed SWITCH model [2]. In contrast to our modeling, they assume a solar PV installation cost about twice as high as for wind, which results in early VRES growth almost exclusively in wind. Subsequently, solar PV costs are assumed to decrease in a steep learning curve, dropping almost down to the cost of onshore wind at the end of their simulation period in 2029. This leads to significant solar installations in later years. Similar to our modeling, VRES installations start with the lowest cost technology, which is complemented by others in the following years, as renewable shares grow. Due to the complexity of the SWITCH model, this analogous development cannot, however, be traced back to the same mechanism of avoiding backup energy needs and surplus production by shifting the mix that we observed in our model.

Note that, since LCOE are minimized for all renewable shares independently, the optimal build-up pathway (white lines in Fig. 3a and b, colored lines in Fig. 3c) sometimes traces an uninstallation or under-usage of previously existing renewable capacity. However, the green region, where LCOE are less than one percent larger than optimal, is broad enough to accommodate a modified pathway that does not include uninstallation. An analogous statement holds for the minimal backup energy pathways, Fig. 2a–c.

3.3. Usage of surplus energy

It can be argued that no value of all occurring surplus energy is an unrealistic assumption. If initially there was no use for surplus electricity, it would be available cheaply. This in turn would strongly incentivize the development of measures to make use of the surplus. A future electricity system is therefore likely to include sources of flexibility to capture some value from surplus generation. For example, demand-side management measures or storage systems may be used, reducing surplus energy. Additionally, inter-FERC region transmission leads to surplus being exported to other parts of the country, where it can be used to replace backup energy. It was found in Ref. [11] that in a 100% renewable scenario, unlimited transmission reduces the residual surplus by roughly one fifth. Another option is to use surplus electricity for heating or transportation.

To address such effects, modified LCOE-minimal pathways are investigated, where only a fraction of the surplus is treated as not giving any gain, thus subtracting only a fraction of the surplus energy from the total generated energy in the denominator of Eq. (5). For example, 20% gain on the surplus could be achieved by recovering the full LCOE of 20% of the surplus by selling it to some alternative consumer (e.g. storage, transmission, synthetic fuel production), or by recovering part of the LCOE on a corresponding larger fraction of the excess generation. The results are illustrated in Fig. 5a and b, again for the AllCA and MISO regions. Shown are three cases where 20%, 40%, and 60% of the incurred LCOE are gained from surplus energy. For AllCA, it is seen that while for the 20% case, not much changes with respect to the no-value-surplus case depicted in Fig. 3a, already 40% of the surplus energy's generation costs gained means a significant shift in the LCOE-minimal path toward the cheaper technology, in this example, solar. However, there is still a significant share of wind power in the 100% LCOE-minimal mix. This changes beyond about 50% of the gains on surplus energy, compare the green lines in Fig. 5c, when the LCOE-minimal mix shifts to solar PV all the way to 100% VRES gross share.

For MISO (Fig. 5b), the absolute shift of the pathways is smaller, because the lower generation cost technology is wind in this case, which brings the backup minimal mix and the LCOE minimal mix closer together from the start. Qualitatively, however, the picture is similar: For 20% and 40% surplus usage, the change in the LCOE-minimal pathway is relatively small. Only for higher surplus usage fractions, the LCOE optimal path finally shifts to 100% wind all the way. This shift toward more wind with growing surplus usage at different VRE gross shares is shown in Fig. 5c (red lines (in web version)). It is seen that for higher gross shares, the LCOE-minimal path reaches 100% wind only at a higher surplus gain than for lower gross shares.

In conclusion, a high share of the surplus energy has to be used for other goals than satisfying the electricity demand to shift the LCOE-minimal mix back to where it is seen on a pure generation-cost basis.

3.4. Sensitivity to different generation costs

As the overall LCOE minimization only depends on the ratio of wind and solar LCOE (compare Eq. (5)), the results remain unchanged as long as wind and solar LCOE are both raised or lowered

by the same percentage. An example of this effect would be observed if learning curves with the same time constants (start time and learning rate) were assumed for both technologies. Such a case is therefore covered by the present work.

Fig. 6a and b shows what happens to Fig. 3a and b when relative cost assumptions change. They depict the LCOE-minimal build-up of wind and solar PV if the initial LCOE are changed such that one technology is \$0.005/kWh more expensive and the other \$0.005/kWh less expensive. While this shifts the least-cost path toward the now cheaper technology, it does not change the qualitative characteristics of the picture as long as the same technology remains the cheaper one. Where solar PV has lower generation costs, the build-up starts with 100% solar PV, and shifts rapidly toward more wind when additional backup needs arise. Where wind is cheaper, the build-up starts with 100% wind, and later gradually includes a small fraction of solar PV. For AllCA, cost changes are small enough such that solar PV remains cheaper for all cost scenarios depicted in Fig. 6a. For MISO, the two different behaviors for lower solar (yellow curve in Fig. 6b) and lower wind generation costs (red and blue curves in Fig. 6b) can be seen.

The changes in these panels when larger cost changes are applied are shown in Fig. 6c, in green for AllCA and in red for MISO.

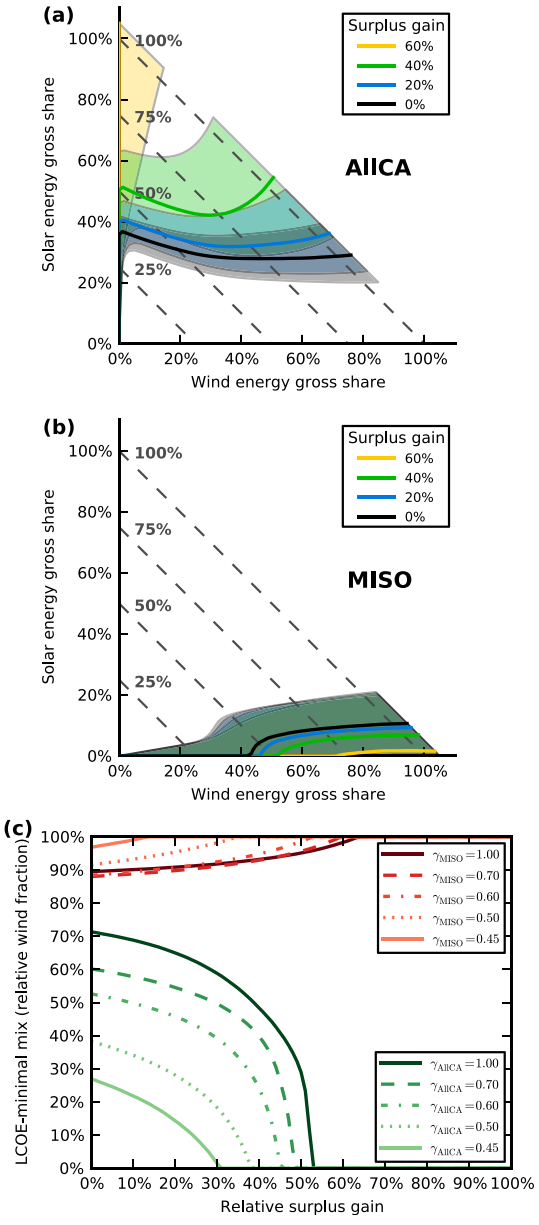

Fig. 5. (a), (b): LCOE-minimizing build-up pathways if it is possible to gain 0 %, 20 %, 40 %, and 60 % of the average LCOE for the surplus energy, for the example regions (a) AllCA and (b) MISO, for wind and solar LCOE of \$0.048/kWh and \$0.036/kWh (in AllCA) or \$0.039/kWh and \$0.041/kWh (in MISO), before accounting for lower-value surplus, respectively. The shadowed regions indicate the 1 pp higher LCOE wind–solar combinations for each surplus gain percentage. (c) shows the LCOE-minimal mix for different VRE gross shares as a function of the surplus gain. The surplus gain can be realized by selling part of the surplus for the normal price, or all of it for a lower than normal price, or something in between.

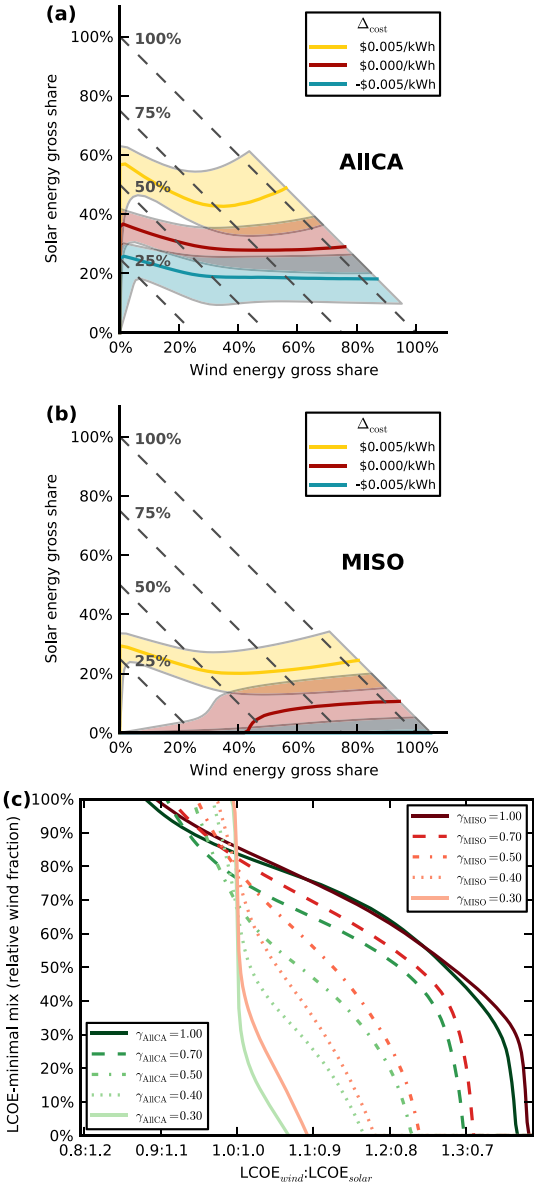

Fig. 6. Cost sensitivity of the least cost build-up pathway for (a) AllCA and (b) MISO. Shown is the effect of cost changes on the optimal pathways, comparing three cases: (1) LCOE (before accounting for no-value surplus) remain unchanged (red curves, Δ_{cost} = \$0.000/kWh in the legend), (2) wind LCOE are reduced by \$0.005/kWh and solar PV LCOE increased by \$0.005/kWh (blue curves, Δ_{cost} = −\$0.005/kWh), and (3) wind LCOE increased by \$0.005/kWh and solar PV LCOE reduced by \$0.005/kWh (Δ_{cost} = \$0.005/kWh). The shaded areas indicate the regions where LCOE are less than 1 % larger than optimal. (c) shows the LCOE-minimal mix as a function of the LCOE ratio, for five different VRE gross shares γ between 30 % and 100 %, for AllCA and MISO. (For interpretation of the references to color in this figure legend, the reader is referred to the web version of this article.)

If LCOE for wind and solar PV are equal, the LCOE-minimal mix equals the backup energy minimizing mix. For lower wind LCOE, wind quickly becomes the only generation technology, while solar PV LCOE have to drop down to less than half of wind LCOE to make a solar PV only mix the cheapest option. This is due to the large mismatch between solar generation alone and the load. For all curves, the sensitivity to initial LCOE becomes lower and lower (curves are less steep) with increasing VRES gross share, because this leads to more surplus/additional backup energy that needs to be minimized besides generation costs. The effects of different resources on these plots are very small, as can be seen from the comparison of AllCA and MISO – the curves for the same gross VRES shares almost coincide in Fig. 6c.

4. Comparison and conclusions

Fig. 4a and c shows that for low VRES gross shares, surplus production entailing additional backup energy needs hardly ever occurs, and thus the choice of the wind/solar mix is largely irrelevant for the backup energy minimization. Starting from a gross share of about 30%, this changes: Surplus production sets in, and hence backup minimization becomes more important, leading to successively narrower minima in backup energy. The wind/solar mix becomes more important with growing installations. In contrast, for the LCOE (Fig. 4b and d), there is a clear minimum for small VRES gross shares on the side of the cheaper technology, in this example figures, solar PV in AllCA and wind in MISO. Once surplus production begins, leading to economically disadvantageous loss of value, the minimal LCOE region starts to shift from lower installation and maintenance costs towards lower surplus production. The effect is mitigated if alternative usages of the surplus energy are found, however, unless more than half of the generation costs of the surplus energy can be recovered in some way, at 100% VRES gross share, the LCOE-minimal mix still includes a significant share of the more expensive technology.

These observations can be interpreted in two ways: First, they can be taken as an indication that while in the beginning of the renewable build-up, least generation costs pathways can be pursued without incurring additional backup energy and subsequently, additional costs, the picture changes drastically as soon as renewable penetrations reach beyond 30%–50%. Then, surplus production becomes an issue, technically as well as economically. One way of tackling this challenge is to examine the backup energy-minimal wind/solar mix and create a mixed renewable portfolio, even if generation costs alone clearly favor only one technology.

Second, the situation can be viewed as a high incentive to make use of (and thus gain from) VRES electricity excess generation. In the example of California with a VRES gross share of 100% and LCOE-minimizing mixes, the minimal LCOE if surplus has no value is almost twice as high as in the case where all surplus earns the same value as grid electricity, cf. Fig. 4b. Surplus usage can be achieved using inter-FERC-regional transmission, storage and demand-side management, and coupling of the electricity system to heating and transportation. A strong transmission grid that effectively allows for long-range aggregation of wind generation is able to smooth it considerably [18–20,23,24], thus providing a better match to the load. It has been shown in Refs. [11,28] that aggregation of load and generation shifts the backup-minimal mix toward a higher wind share, and results in a reduction of backup energy needs by about 20% in the contiguous US.

In wind-rich Ireland, a study has shown that wind integration can furthermore be aided with flexible loads and hydro power plants, reporting a possible surplus-free integration of 38% wind into the Irish grid [29].

Solar PV integration benefits much from short-term storage, which shifts the backup-minimal mix towards solar PV [30]. An alternative to solar PV combined with storage is concentrated solar power with inherent heat storage.

Going beyond integration measures within the electricity sector, remaining electrical excess generation can be used for heating or to produce CO_2-neutral synthetic fuels for aviation and road transport. This would lead to a strong coupling of future energy infrastructures across the three big energy sectors electricity, heating and cooling, and transportation.

Acknowledgments

SB gratefully acknowledges financial support from O. and H. Stöcker as well as M. and H. Puschmann, BAF from a National Defense Science and Engineering Graduate (NDSEG) fellowship, a National Science Foundation (NSF) graduate fellowship, and a Stanford University Charles H. Leavell Graduate Student Fellowship, and GBA from DONG Energy and the Danish Advanced Technology Foundation. Furthermore, SB thanks the HGS-HIRe graduate school for the abroad grant to visit Stanford University. The project underlying this report was supported by the German Federal Ministry of Education and Research under grant no. 03SF0472C. The responsibility for the contents lies with the authors.

References

[1] Budischak C, Sewell D, Thomson H, Mach L, Veron DE, Kempton W. Cost-minimized combinations of wind power, solar power and electrochemical storage, powering the grid up to 99.9% of the time. J Power Sources 2013;225(0):60–74. http://dx.doi.org/10.1016/j.jpowsour.2012.09.054.
[2] Nelson J, Johnston J, Mileva A, Fripp M, Hoffman I, Petros-Good A, et al. High-resolution modeling of the western North American power system demonstrates low-cost and low-carbon futures. Energy Policy 2012;43(0):436–47. http://dx.doi.org/10.1016/j.enpol.2012.01.031.
[3] Williams JH, DeBenedictis A, Ghanadan R, Mahone A, Moore J, Morrow WR, et al. The technology path to deep greenhouse gas emissions cuts by 2050: the pivotal role of electricity. Science 2012;335:53–9. http://dx.doi.org/10.1126/science.1208365.
[4] Hart EK, Jacobson MZ. A Monte Carlo approach to generator portfolio planning and carbon emissions assessments of systems with large penetrations of variable renewables. Renew Energy 2011;36(8):2278–86. http://dx.doi.org/10.1016/j.renene.2011.01.015.
[5] Hand M, Baldwin S, DeMeo E, Reilly J, Mai T, Arent D, et al. In: Renewable electricity futures study, vol. 4; 2012. http://www.nrel.gov/analysis/re_futures/. NREL/TP-6A20–52409.
[6] McKinsey & Company, KEMA, The Energy Futures Lab at Imperial College London, Oxford Economics, ECF. Roadmap 2050–a practical guide to a prosperous, low-carbon Europe. Tech. Rep. European Climate Foundation; 2010. http://www.roadmap2050.eu/. Online, accessed June 2012
[7] Fürsch M, Hagspiel S, Jägemann C, Nagl S, Lindenberger D, Glotzbach L, et al. Roadmap 2050 – a closer look. Tech. Rep.. energynautics and Institute for Energy Economy at the University of Cologne. 2011. http://www.energynautics.com/news/
[8] Gelman R. 2012 renewable energy data book. Tech. Rep. US Department of Energy. 2013. Online available from:, http://www.nrel.gov/news/press/2013/5302.html. retrieved Sep 2014.
[9] Jacobson MZ, Delucchi MA. Providing all global energy with wind, water, and solar power, part I: technologies, energy resources, quantities and areas of infrastructure, and materials. Energy Policy 2011;39(3):1154–69. http://dx.doi.org/10.1016/j.enpol.2010.11.040.
[10] Delucchi MA, Jacobson MZ. Providing all global energy with wind, water, and solar power, part II: reliability, system and transmission costs, and policies. Energy Policy 2011;39(3):1170–90. http://dx.doi.org/10.1016/j.enpol.2010.11.045.
[11] Becker S, Frew BA, Andresen GB, Zeyer T, Schramm S, Greiner M, et al. Features of a fully renewable US electricity system: optimal mixes of wind and solar PV and transmission grid extensions. Energy 2014a;72:443–58. Online at: http://dx.doi.org/10.1016/j.energy.2014.05.067. http://arxiv.org/abs/1402.2833. preprint available at:.
[12] Corcoran BA, Jenkins N, Jacobson MZ. Effects of aggregating electric load in the United States. Energy Policy 2012;46:399–416. http://dx.doi.org/10.1016/j.enpol.2012.03.079.
[13] Saha Suranjana, Moorthi Shrinivas, Pan Hua-Lu, Wu Xingreni, Wang Jiande, Nadiga Sudhir, et al. The NCEP climate forecast system reanalysis. Bull Amer

Meteor Soc 2010;91(8):1015–57. http://dx.doi.org/10.1175/2010BAMS3001.1.
[14] Andresen GB, Søndergaard AA, Greiner M. Validation of Danish wind time series from a new global renewable energy atlas for energy system analysis. Submitted for review 2014. Preprint available at: http://arxiv.org/abs/1409.3353.
[15] Søndergaard AA. Development of a renewable energy atlas and extreme event analysis in renewable energy systems. M. Sc. thesis. Denmark: Aarhus University; 2013.
[16] Potter C, Nijssen B. Development of regional wind resource and wind plant output datasets. Tech. Rep.. 3TIER, for NREL, under supervision of D. Seattle, Washington: Lew; 2009. Final data sets available from: http://www.nrel.gov/electricity/transmission/western_wind_dataset.html
[17] Brower M. Development of eastern regional wind resource and wind plant output datasets. Tech. Rep.. AWS truewind LLC, for NREL, under supervision of D. Albany, New York: Corbus; 2009. Final data sets available from: http://www.nrel.gov/electricity/transmission/eastern_wind_dataset.html
[18] Archer CL, Jacobson MZ. Supplying baseload power and reducing transmission requirements by interconnecting wind farms. J Appl Meteorol Climatol 2007;46(11):1701–17. http://dx.doi.org/10.1175/2007JAMC1538.1.
[19] Holttinen H. Impact of hourly wind power variations on the system operation in the Nordic countries. Wind Energy 2005;8(2):197–218. http://dx.doi.org/10.1002/we.143.
[20] Sinden G. Characteristics of the UK wind resource: long-term patterns and relationship to electricity demand. Energy Policy 2007;35(1):112–27. http://dx.doi.org/10.1016/j.enpol.2005.10.003.
[21] Wiemken E, Beyer H, Heydenreich W, Kiefer K. Power characteristics of PV ensembles: experiences from the combined power production of 100 grid connected PV systems distributed over the area of Germany. Sol Energy 2001;70(6):513–8. http://dx.doi.org/10.1016/S0038-092X(00)00146-8.
[22] Mills A, Wiser R. Implications of wide-area geographic diversity for short-term variability of solar power. Tech. Rep. Lawrence Berkeley National Laboratory; 2010
[23] Widén J. Correlations between large-scale solar and wind power in a future scenario for Sweden. IEEE Trans Sustain Energy 2011;2(2):177–84. http://dx.doi.org/10.1109/TSTE.2010.2101620.
[24] Kempton W, Pimenta FM, Veron DE, Colle BA. Electric power from offshore wind via synoptic-scale interconnection. Proc Natl Acad Sci 2010;107(16):7240–5. http://dx.doi.org/10.1073/pnas.0909075107.
[25] Tech. Rep. Energy and Environmental Economics. Cost and performance review of generation technologies: recommendations for WECC 10- and 20-year studies. San Francisco, CA: E3; 2012. Online available from: http://www.nwcouncil.org/media/6867814/E3_GenCapCostReport_finaldraft.pdf. retrieved Aug 2013
[26] US Army Corps of Engineers. Civil works construction cost index system. Tech. Rep.. US army corps of engineers. 2011. http://planning.usace.army.mil/toolbox/library/EMs/em1110.2.1304.pdf. Online, accessed Aug 2013
[27] Lazard. Lazard's levelized cost of energy analysis–version 8.0. 2014.
[28] Becker S, Rodríguez RA, Andresen GB, Schramm S, Greiner M. Transmission grid extensions during the build-up of a fully renewable pan-European electricity supply. Energy 2014b;64:404–18. http://dx.doi.org/10.1016/j.energy.2013.10.010. http://arxiv.org/abs/1307.1723. preprint available from:.
[29] EirGrid. All island grid study. 2008. Online available from: http://www.eirgrid.com/renewables/all-islandgridstudy/. retrieved Sep 2014.
[30] Rasmussen MG, Andresen GB, Greiner M. Storage and balancing synergies in a fully or highly renewable pan-European power system. Energy Policy 2012;51:642–51. http://dx.doi.org/10.1016/j.enpol.2012.09.009.